Scaling of Static Fracture of Quasi-Brittle Structures: Strength, Lifetime, and Fracture Kinetics

Jia-Liang Le[1]
Assistant Professor
Department of Civil Engineering,
University of Minnesota,
Minneapolis, MN 55455

Zdeněk P. Bažant[2]
McCormick Institute Professor and
W.P. Murphy Professor
of Civil Engineering
and Materials Science,
Northwestern University,
2145 Sheridan Rd., CEE,
Evanston, IL 60208
e-mail: z-bazant@northwestern.edu

The paper reviews a recently developed finite chain model for the weakest-link statistics of strength, lifetime, and size effect of quasi-brittle structures, which are the structures in which the fracture process zone size is not negligible compared to the cross section size. The theory is based on the recognition that the failure probability is simple and clear only on the nanoscale since the probability and frequency of interatomic bond failures must be equal. The paper outlines how a small set of relatively plausible hypotheses about the failure probability tail at nanoscale and its transition from nano- to macroscale makes it possible to derive the distribution of structural strength, the static crack growth rate, and the lifetime distribution, including the size and geometry effects [while an extension to fatigue crack growth rate and lifetime, published elsewhere (Le and Bažant, 2011, "Unified Nano-Mechanics Based Probabilistic Theory of Quasibrittle and Brittle Structures: II. Fatigue Crack Growth, Lifetime and Scaling," J. Mech. Phys. Solids, 1322–1337), is left aside]. A salient practical aspect of the theory is that for quasi-brittle structures the chain model underlying the weakest-link statistics must be considered to have a finite number of links, which implies a major deviation from the Weibull distribution. Several new extensions of the theory are presented: (1) A derivation of the dependence of static crack growth rate on the structure size and geometry, (2) an approximate closed-form solution of the structural strength distribution, and (3) an effective method to determine the cumulative distribution functions (cdf's) of structural strength and lifetime based on the mean size effect curve. Finally, as an example, a probabilistic reassessment of the 1959 Malpasset Dam failure is demonstrated. [DOI: 10.1115/1.4005881]

Introduction

Modern engineering structures are often made of quasi-brittle materials. These are brittle heterogeneous materials which include concrete (as the archetypical example), rocks, coarse-grained and toughened ceramics, fiber composites, masonry, mortar, stiff cohesive soils, grouted soils, consolidated snow, wood, paper, rigid foams, sea ice, dental ceramics, dentine, bone, biological shells, many bio and bio-inspired materials, and many more materials at the micro- and nanoscales. The salient feature of quasi-brittle structures is that the size of material inhomogeneities is not negligible compared to the structure size. This causes the quasi-brittle structures to exhibit a size-dependent failure behavior: small-size structures fail in a quasi-plastic manner, whereas large-size structures fail in a brittle manner. Such a transition has been well demonstrated by the analysis of size effect on the mean structural strength [1–5].

Recent research efforts have been directed to the probabilistic aspect of structural strength of quasi-brittle structures, which is more complicated compared to ductile and brittle structures [6–9]. Here the attention is limited to a broad class of structures that fail at the initiation of a macrocrack from one representative volume element (RVE), whose size is about 2 to 3 times of the size of material inhomogeneities. Statistically, the structure must follow the weakest-link model which allows the cumulative distribution function (cdf) of structural strength to be calculated from the cdf of the strength of one RVE.

The strength distribution of one RVE can further be related to the strength cdf of a nano scale element through a multiscale statistical model, where the strength statistics of the nanoscale element is derived from atomistic fracture mechanics of nanocracks propagating by small, activation-energy-controlled, random jumps through the nanoscale structure [8]. The model predicts that the cdf of structural strength depends on the structure size; as the size increases, there is a gradual transition from the Gaussian (or normal) distribution (modified by a far-left power-law tail) to the Weibull distribution (which should properly be called the Fisher-Tippett-Weibull distribution [10]). Consequently, the model implies an intricate size effect on the mean structural strength, which agrees with the predictions by other well-established mechanical models such as nonlocal Weibull theory and cohesive crack model [7].

This finite weakest-link model of strength distribution has further been extended to the lifetime distribution of quasi-brittle structures under constant loads by means of kinetics of crack growth [8,9]. The crack growth rate law under constant loading was first studied in the context of corrosive environment based on the classical rate process theory [11,12]. For purely stress-driven crack growth, experiments showed that the dependence of crack growth velocity on the applied stress could be described by a simple power law [13–15]. Fett [16] suggested that the power law for crack growth rate could be justified by the breakage frequency of the bond between a pair of atoms. However, such a justification is limited to the Morse potential only, and it does not take into account the bridging between the atomic scale and the macroscale. A recent study showed that the power law for crack growth rate could be justified on the basis of fracture mechanics of nanocrack propagation and the equality of energy dissipation rates calculated on the nano- and macroscales [8,17]. Based on the crack growth kinetics, the lifetime distribution can then be derived from the

[1]Formerly Graduate Research Assistant, Northwestern University.
[2]Corresponding author.

Contributed by the Applied Mechanics of ASME for publication in the JOURNAL OF APPLIED MECHANICS. Manuscript received July 1, 2011; final manuscript received January 13, 2012; accepted manuscript posted February 9, 2012; published online April 4, 2012. Assoc. Editor: Huajian Gao.

strength distribution. It has been shown that the resulting lifetime cdf agrees well with the observed lifetime histograms of quasi-brittle materials, such as engineering and dental ceramics [9,17,18]. For an explanation why the present model eschews flaw statistics see [9].

This paper reviews the recently developed finite weakest-link model of strength and lifetime distributions and presents three new extensions of the theory: (1) a derivation of the dependence of static crack growth rate on the structure size and geometry, (2) an approximate closed-form solution for the cdf of strength, and (3) an effective method for determining the strength and lifetime cdf's based on the mean size effect curves. A probabilistic reassessment of the failure of the Malpasset Dam is presented as an example. The writers' presentation at the Rice Symposium further included an extension of the present theory to fatigue crack growth and to size effect on the distribution of fatigue lifetime. But this aspect has been treated in another paper [19].

Stress-Driven Fracture of Nanoscale Structures

Failure of a macrostructure always originates from the fracture of its nanostructures, such as a regular atomic lattice representing a single crystal grain of brittle ceramic, or a completely disordered structure representing a system of nanoparticles of the calcium silicate hydrate in concrete. Therefore, the statistics of macrostructural failure should be derived from the fracture statistics at the nanoscale.

Extensive efforts have been devoted to physically based numerical simulations of crack propagation through an atomic lattice, based on the coupling between the quantum mechanics (QM) and molecular dynamics (MD) [20,21]. Nevertheless, it requires millions of QM-MD simulations to obtain the tail part of failure probability, which is currently beyond the conventional computational capacity. Despite the limitations of computational approach for the failure statistics of nanostructures, there exists a well established physical theory for the frequency of breakage of interatomic bonds. It is the rate process theory in which the rates of breakage of interatomic bonds are derived from the distribution of thermal energies of atoms and the frequency of passage over the activation energy barriers of the interatomic potential [22–27]. This theory justifies the Arrhenius thermal factor and has long been used to transit from the atomic scale to the material scale, providing the temperature and stress dependence of the rates of creep, diffusion, phase changes, adsorption, chemical reactions, etc.

The frequency of interatomic bond breakage can further be considered to be equal to the breakage probability. This is due to the fact that the process at the atomic scale is quasi-stationary, which can be verified in two ways: (1) The natural energy scale for chemical bonds and activation barriers between long-lived well-defined molecular states, is the electron-volt. This scale is larger by at least an order of magnitude than the thermal energy scale ($kT = 0.25$ eV at room temperature, where $k =$ Boltzmann constant and $T =$ absolute temperature), while in the case of a large free energy barrier the transition between two states is relatively slow, making the breakage process quasi-stationary. (2) The interatomic bonds in the fracture process zone (FPZ) break at the rate of about 10^5/s in static fracture and about 10^{10}/s in fracture under missile impact, while the rate of thermal atomic vibrations is about 10^{14}/s. Therefore, one jump over the activation energy barrier, or one interatomic bond break, occurs only after every 10^9 or 10^4 atomic vibrations, respectively.

Consider a nanocrack propagating through a nanoelement, either a regular atomic lattice or a disordered system of nanoparticles (Fig. 1). There are many pairs of interatomic bonds or many nanoparticle connections along this nanocrack, and the nanocrack advances in discrete jumps over the activation barriers of these interatomic bonds or nanoparticle connections. The nanoelement fails when the nanocrack propagates to a certain critical length, which involves many discrete crack front jumps. Therefore, the energy difference ΔQ between two adjacent potential wells, which represents two adjacent metastable states, must be very small compared to the activation energy barrier Q_0.

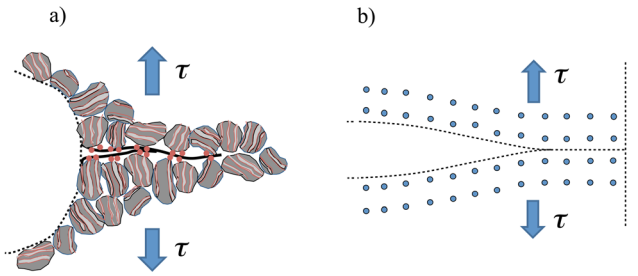

Fig. 1 Facture of a nanoscale element (*a*) disordered nanoparticle network and (*b*) atomic lattice block [19]

For the case of a large activation barrier ($Q_0 >> \Delta Q$), the rate of transition between two adjacent metastable states can be expressed by Kramers' formula [24,28,29]:

$$f_1 = \nu_T\left(e^{(-Q_0+\Delta Q/2)/kT} - e^{(-Q_0-\Delta Q/2)/kT}\right) = 2\nu_T e^{-Q_0/kT}\sinh[\Delta Q/2kT] \tag{1}$$

where $Q_0 =$ free activation energy barrier, $\nu_T = kT/h$, $h = 6.626 \times 10^{-34}$ J s = Planck constant = (energy of a photon)/(frequency of its electromagnetic wave), and $\Delta Q =$ energy difference between two adjacent states. The breakage frequency, which is equal to the breakage probability, can be calculated as $f_b = f_1/f_0$, where $f_0 =$ rate of thermal atomic vibrations. In the present model, the two adjacent states represent the states of a nanoelement before and after the nanocrack front propagates by one atomic spacing or one spacing of nanoparticle connections. Therefore, ΔQ can further be related to the applied remote stress τ through the equivalent linear elastic fracture mechanics [8]:

$$\Delta Q = V_a(\alpha)\frac{\tau}{E_1} \tag{2}$$

where $V_a(\alpha) = \delta_a(\gamma_1\alpha l_a^2)k_a^2(\alpha) =$ activation volume, $\delta_a =$ atomic spacing or spacing of nano-particle connections, $k_a(\alpha) =$ dimensionless stress intensity factor of nanoelement, $l_a =$ characteristic dimension of the nanoelement, $\alpha =$ relative crack length $= a/l_a$ ($a =$ equivalent crack length based on the equivalent linear elastic fracture mechanics), and $\gamma_1 =$ geometry constant such that $\gamma_1 a =$ perimeter of the growing crack front. The nanoscale stress τ can be considered proportional to the macroscale stress σ, i.e., $\tau = c\sigma$, where $c =$ constant.

At the nanoscale, the breakage of individual interatomic bonds or nanoparticle connections can be considered as an independent process [26]. Consequently, the frequency of failure of a nanoelement can be calculated as the sum of the frequencies of breakage of interatomic bonds or nanoparticle connections that are needed to propagate the nanocrack to its critical length. Furthermore, previous studies [8,9] have demonstrated that the argument of the sine hyperbolic function in Eq. (1) is usually very small, i.e., $\Delta Q/2kT < 0.1$. Based on Eqs. (1) and (2), we can thus write the failure probability of the nanoelement under stress τ as follows:

$$P_f \propto \nu_T e^{-Q_0/kT}\left[\int_{\alpha_0}^{\alpha_c} V_a(\alpha)d\alpha\right]\frac{c^2\sigma^2}{E_1 kT} \tag{3}$$

Based on the present framework, the velocity of nanocrack propagation can simply be calculated as [17]

$$v_a = f_1\delta_a = \nu_1 e^{-Q_0/kT}K_a^2 \tag{4}$$

where $\nu_1 = \delta_a^2(\gamma_1\alpha l_a)/E_1 h$ and $K_a =$ stress intensity factor (SIF) of the nanoelement. The exponent value of 2 ensues from the

transition rate theory upon noting that the energy difference (or bias) between the forward and backward activation energies (i.e., between two adjacent metastable states of crack front in a discrete nanostructure) must be proportional to the nanoscale energy release rate according to the equivalent linear elastic fracture mechanics, which in turn is proportional to the square of the applied nanostress.

Note that the foregoing analysis is limited to the stress-driven failure. When the stress is sufficiently small, the diffusion-driven failure would govern [30]. However, a simplified one-dimensional random walk analysis showed that the diffusion-driven failure would correspond to an extremely low failure probability $\propto 10^{-12}$), which is not of interest in most practical engineering designs [9,17].

Probability Distribution of Structural Strength

To link the strength statistics at nanoscale and macroscale, one must rely on a certain multiscale transition framework. Direct numerical simulations are often associated with two main difficulties: (1) A questionable assumption about how physical laws transit across the scales, and (2) excessive computational efforts for simulating the tail of strength cdf. Instead of numerical multiscale simulations, recent studies showed that the strength distribution of a macroscale RVE can be approximately related to the strength distribution of its nanoelements through a hierarchical statistical model [7–9], which consists of a bundle of only two long subchains, each of which consists of subbundles of two sub-subchains, each of which consists of sub-subbundles, etc., until the nanoscale element is reached (see Fig. 3(*c*) in [9]). Although the hierarchical model merely represents a mathematical approximation of multiscale transition of strength statistics, it qualitatively reflects two main physical mechanisms of the failure of quasi-brittle materials, namely distributed damage and damage localization.

The mathematical formulations of chain and bundle models have been discussed in detail, e.g., [7,9,31–36]. A recent study [7,9] showed that the probability distribution function of RVE strength could be approximated as a Gaussian distribution onto which a power-law tail is grafted at the probability $P_{gr} \approx 10^{-4}$–10^{-3}:

$$p_1(\sigma_N) = (m/s_0)(\sigma_N/s_0)^{m-1} e^{-(\sigma_N/s_0)^m} \quad (\sigma_N \le \sigma_{gr}) \tag{5}$$

$$p_1(\sigma_N) = r_f e^{-(\sigma'_N-\mu_G)^2/2\delta_G^2}/\delta_G\sqrt{2\pi} \quad (\sigma_N \le \sigma_{gr}) \tag{6}$$

where $p_1(\sigma_N)$ = probability density function (pdf), σ_N = nominal strength, which is a maximum load parameter with the dimension of stress. In general, $\sigma_N = c_n P_{max}/bD$ or $c_n P_{max}/D^2$ for two- or three-dimensional scaling (P_{max} = maximum load of the structure, c_n = parameter chosen such that σ_N represent the maximum principal stress in the structure, b = structure thickness in the third dimension, D = characteristic structure dimension or size). Furthermore, m (Weibull modulus) and s_0 are the shape and scale parameters of the Weibull tail, and μ_G and δ_G are the mean and standard deviation of the Gaussian core if considered extended to $-\infty$, r_f is a scaling parameter required to normalize the grafted cdf such that $\int_0^\infty p_1(\sigma_N)d\sigma_N = 1$. Finally, continuity of the pdf at the grafting point requires that $p_1(\sigma_{gr}^+) = p_1(\sigma_{gr}^-)$.

Since we limit our attention to structures failing (under controlled load) at the initiation of a macrorack from one RVE, the structure can be statistically modeled as a chain of RVEs. Based on the joint probability theorem and the assumption that the strength of each RVE is an independent random variable, the strength cdf of the structure can be calculated as

$$P_f(\sigma_N) = 1 - \prod_{i=1}^{N} \{1 - P_1[\langle \sigma_N s(x_i)\rangle]\} \tag{7}$$

where $s(\boldsymbol{x}_i)$ = dimensionless stress field such that $\sigma_N s(\boldsymbol{x}_i)$ = maximum principal stress for ith RVE, P_1 = strength cdf of one RVE, and $\langle x\rangle = \max(x, 0)$. What governs the cdf of strength of very large structures is the tail part of the strength cdf of one RVE, and in that case Eq. (7) leads to the classical two-parameter Weibull distribution [7], which is consistent with the extreme value statistics for the strength cdf of perfectly brittle materials [37–40]:

$$P_f(\sigma_N) = 1 - \exp\left[-N_{eq}(\sigma_N/s_0)^m\right] \tag{8}$$

where $N_{eq} = \int_V \langle s(\boldsymbol{x})\rangle^m dV(\boldsymbol{x})/l_0^3$ = equivalent number of RVEs and l_0 = RVE size. N_{eq} physically means that a chain of N_{eq} RVEs under a uniform stress σ_N would give the same failure probability as Eq. (7) for a body with nonuniform stress field $\sigma_N s(\boldsymbol{x})$. Clearly the concept of N_{eq} leads to a closed-form expression of the strength cdf in terms of the stress field. However, for small- and intermediate-size structures, N_{eq} cannot be expressed as an explicit function of the stress field. In such case, one has to rely on the original weakest-link model [Eq. (7)].

Recent studies suggested a nonlocal boundary layer model to calculate the strength cdf of structures of any size [41]. In this method, a boundary layer of thickness $h_0 \approx l_0$ along all the surfaces is separated from the structure. For the boundary layer, one only needs to evaluate the stress for the points of the middle surface Ω_M of the layer. For the interior domain V_I, the failure probability of each material point is considered to depend on the nonlocal stress. Therefore, the original weakest-link model can be rewritten as

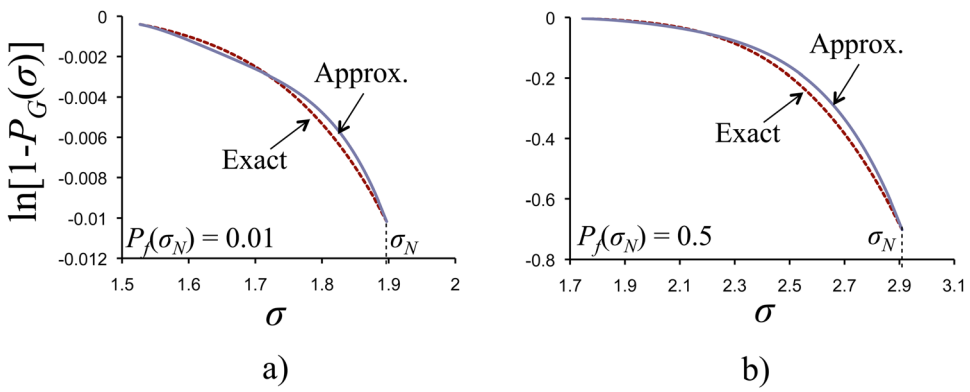

Fig. 2 Approximation of grafted Weibull-Gaussian cdf of strength by the Taylor series expansion

$$ln(1-P_f) = h_0 \int_{\Omega_M} ln\{1-P_1[\sigma(\boldsymbol{x}_M)]\}\frac{d\Omega(\boldsymbol{x}_M)}{V_0} + \int_{V_I} ln\{1-P_1[\bar{\sigma}(\boldsymbol{x})]\}\frac{dV(\boldsymbol{x})}{V_0} \quad (9)$$

where $\bar{\sigma}(\boldsymbol{x})$ = nonlocal stress = $\int_V w(\boldsymbol{x}-\boldsymbol{x}')\sigma(\boldsymbol{x}')\mathrm{d}V(\boldsymbol{x}')$ and $w(\boldsymbol{x}-\boldsymbol{x}')$ = weighting function [10,41]. The main advantage of the nonlocal boundary layer model is that it allows one to compute the strength cdf without subdividing the structure into the RVEs. However, it does not lead to a closed-form expression for the cdf of structural strength.

To obtain an approximate closed-form solution for the strength cdf, the following approach is proposed here: Divide further both the boundary layer Ω_M and the interior part V_I into two parts: (1) the Weibullian region, where the principal stress is less than the grafting stress, and (2) the Gaussian region, where the principal stress is larger than the grafting stress. Then one could rewrite Eq. (9) as

$$ln(1-P_f) = \underbrace{\int_{V_W} ln[1-P_W(\bar{\sigma}(\boldsymbol{x}))]\frac{dV_W(\boldsymbol{x})}{l_0^3}}_{I_{V_W}} + \underbrace{\int_{V_G} ln[1-P_G(\bar{\sigma}(\boldsymbol{x}))]\frac{dV_G(\boldsymbol{x})}{l_0^3}}_{I_{V_G}} + \underbrace{\int_{\Omega_W} ln[1-P_W(\sigma(\boldsymbol{x}))]\frac{d\Omega_W(x)}{l_0^2}}_{I_{\Omega_W}} + \underbrace{\int_{\Omega_G} ln[1-P_G(\sigma(\boldsymbol{x}))]\frac{d\Omega_G(\boldsymbol{x})}{l_0^2}}_{I_{\Omega_G}} \quad (10)$$

where P_W = Weibull tail of strength cdf of one RVE, P_G = Gaussian part of strength cdf of one RVE, V_W = Weibullian region of the interior part of structure = $\{\boldsymbol{x} \mid \boldsymbol{x} \in V_I \wedge \bar{\sigma}(\boldsymbol{x}) \le \sigma_{\mathrm{gr}}\}$, V_G = Gaussian region of the interior part of structure = $\{\boldsymbol{x} \mid \boldsymbol{x} \in V_I \wedge \bar{\sigma}(x) > \sigma_{\mathrm{gr}}\}$, Ω_W = Weibullian region of the boundary layer = $\{\boldsymbol{x} \mid \boldsymbol{x} \in \Omega_M \wedge \sigma(x) \le \sigma_{\mathrm{gr}}\}$, and Ω_G = Gaussian part of the boundary layer = $\{\boldsymbol{x} \mid \boldsymbol{x} \in \Omega_M \wedge \sigma(\boldsymbol{x}) > \sigma_{\mathrm{gr}}\}$.

The integrals for the Weibullian region I_{V_W} and I_{Ω_W} can easily be expressed as a function of the stress field by using the concept of N_{eq} [Eq. (8)]. Though the integrals I_{V_G} and I_{Ω_G} for the Gaussian region cannot be explicitly related to the stress field, an approximate solution is possible based on the Taylor expansion of the Gaussian part of the grafted distribution of RVE strength. The weakest-link model implies that the material elements subjected to small principal stress make negligible contributions to the failure of the entire structure (to illustrate it, consider the Weibull distribution with the Weibull modulus of 24; then, if the failure probability of an element with principal stress σ is p, then the failure probabilities of the elements with principal stress 0.8σ, 0.6σ, and 0.4σ are about $4.7\times10^{-3}p$, $4.7\times10^{-6}p$, and $2.8\times10^{-10}p$, respectively).

Therefore, to calculate the cdf of strength, one could simply consider the elements with principal stress larger than $0.6\sigma_N$. With such a limited stress range, one could approximate $\ln[1-P_G(\sigma)]$ by a linear combination of the Taylor expansions of $\ln[1-P_G(\sigma)]$ at $\sigma=\sigma_N$ and $\sigma=\mu\sigma_N$, where $\mu=\max(0.6, \sigma_{\mathrm{gr}}/\sigma_N)$:

$$\ln[1-P_G(\sigma)] = \phi(\sigma)\sum_{k=0}^{3}\frac{f^{(k)}(\mu\sigma_N)}{k!}(\sigma-\mu\sigma_N)^k + [1-\phi(\sigma)]\sum_{k=0}^{3}\frac{f^{(k)}(\sigma_N)}{k!}(\sigma-\sigma_N)^k \quad (11)$$

$$\text{where} \quad f^{(k)}(\sigma) = \frac{\mathrm{d}^k \ln[1-P_G(\sigma)]}{\mathrm{d}\sigma^k} \quad (12)$$

$$\phi(\sigma) = 1 - \left[\frac{\sigma-\mu\sigma_N}{\sigma_N-\mu\sigma_N}\right]^2 \quad (13)$$

Figure 2 shows that the foregoing approximation based on the Taylor series expansion agrees well with the exact behavior of $\ln[1-P_G(\sigma)]$. With Eq. (11), the integrals I_{V_G} and I_{Ω_G} can then be explicitly related to the stress field:

$$I_{V_G}(\mu) = \sum_{k=0}^{3}\frac{f^{(k)}(\mu\sigma_N)}{k!}\Delta_{V_G,1}(k,\mu) + \sum_{k=0}^{3}\frac{f^{(k)}(\sigma_N)}{k!}\Delta_{V_G,2}(k,\mu) \quad (14)$$

$$I_{\Omega_G}(\mu) = \sum_{k=0}^{3}\frac{f^{(k)}(\mu\sigma_N)}{k!}\Delta_{\Omega_G,1}(k,\mu) + \sum_{k=0}^{3}\frac{f^{(k)}(\sigma_N)}{k!}\Delta_{\Omega_G,2}(k,\mu) \quad (15)$$

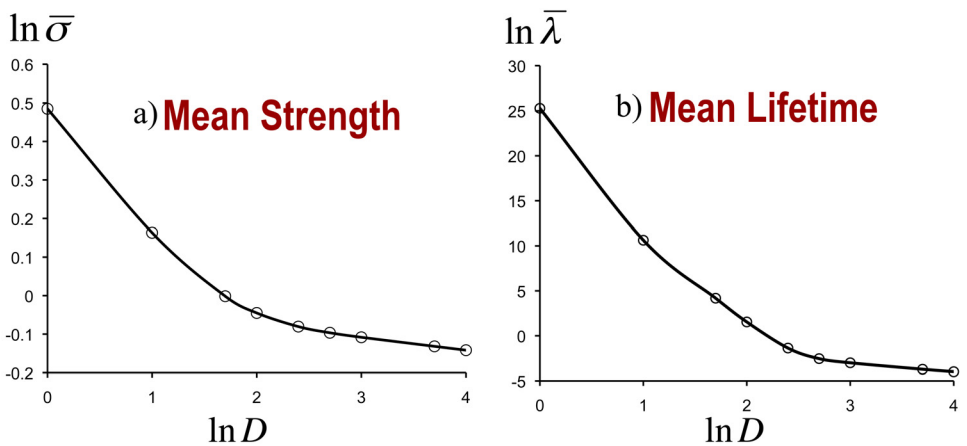

Fig. 3 Mean size effects on structural strength and lifetime

$$\Delta_{V_G,1}(k,\mu)=\frac{1}{l_0^3}\int_{V_G(\mu)}\left[1-\left(\frac{\bar{s}(\boldsymbol{x})-\mu}{1-\mu}\right)^2\right][\bar{s}(\boldsymbol{x})-\mu]^k dV_G \quad (16)$$

$$\Delta_{V_G,2}(k,\mu)=\frac{1}{l_0^3(1-\mu)^2}\int_{V_G(\mu)}[\bar{s}(\boldsymbol{x})-\mu]^2[\bar{s}(\boldsymbol{x})-\mu]^k dV_G \quad (17)$$

$$\Delta_{\Omega_G,1}(k,\mu)=\frac{1}{l_0^2}\int_{\Omega_G(\mu)}\left[1-\left(\frac{s(\boldsymbol{x})-\mu}{1-\mu}\right)^2\right][s(\boldsymbol{x})-\mu]^k d\Omega_G \quad (18)$$

$$\Delta_{\Omega_G,2}(k,\mu)=\frac{1}{l_0^2(1-\mu)^2}\int_{\Omega_G(\mu)}[s(\boldsymbol{x})-\mu]^2[s(\boldsymbol{x})-1]^k d\Omega_G \quad (19)$$

$\Delta_{V_G}(k,\mu)$ and $\Delta_{\Omega_G}(k,\mu)$ can be analytically integrated for structures with some simple stress field, such as linear and bilinear stress profiles. This is probably applicable to many structures where the profile of the stress field in proximity of the point with the largest maximum principal stress can be approximated by a linear function. By expressing the strength cdf in a closed form, one could then easily calibrate the statistical parameters based on the optimum fits of experimentally measured histograms.

Kinetics of Static Crack Growth

Besides structural strength, the service lifetime of structures under a prescribed constant load is another important design consideration. The kinetics of static crack growth has long been recognized as the proper way to calculate the structural lifetime [8,26,42,43]. Equation (4) shows that the growth rate of a nanocrack can be expressed as a power-law function of the SIF of the nanoelement, and that the exponent must be 2. Extensive experiments showed that the crack growth rate at the macroscale also has a power-law dependence on the SIF [13,14]:

$$\dot{a}=\frac{da}{dt}=AK^n \quad (20)$$

where $a=$ macrocrack length, $K=$ stress intensity factor (SIF), and A, n are empirical parameters to be calibrated.

As the macrocrack grows, there is a finite FPZ attached to the crack tip. In a recent study [8,9,17], it has been shown that the power-law form for macrocrack growth could be physically justified by equating the energy dissipation rate associated with the macrocrack growth to the sum of energy dissipation rates of all the active nanocracks in the macroscale FPZ, i.e.,

$$\mathcal{G}\dot{a}=\sum_{i=1}^{Na}\mathcal{G}_i\dot{a}_i \quad (21)$$

where $\mathcal{G}$ and $\mathcal{G}_i$ denote the energy release rate functions for the macrocrack a and nanocracks a_i ($i=1, 2, 3\ldots$), respectively, and $N_a=$ number of active nanocracks in the FPZ. Upon substituting Eq. (4) into $\dot{a}_i$ and averaging the energy dissipation rates of all the nanocracks, one gets

$$\dot{a}=e^{-Q_0/kT}Na\frac{\nu_a K_a^4 E}{E_a K^2} \quad (22)$$

where $E=$ Young's modulus of macrostructure, $E_a=$ average Young's modulus of a nano element, $K_a=$ average SIF of a nanoelement, and $\nu_a=$ average of all ν_i. The SIFs at macro- and nanoscales must be proportional, i.e., $K=\omega K_a$, where $\omega=$ constant.

The number of active nanocracks N_a can be calculated based on a hierarchy of FPZs at different scales [8]. One could consider that the macroscale FPZ contains n_1 microcracks, each of which has its own FPZ which contains n_2 subscale cracks, each of which has its own FPZ, etc., all the way to the nanoscale. For the nanoscale cracks, nonlinear behavior at the crack tip is governed not by a FPZ of a finite width but by a cohesive line crack characterized by the potentials of a row of interatomic bonds or nanoparticle connections (e.g., [44]). Therefore, if there are q different scales between the macro- and nanoscales, then $N_a=n_1n_2\ldots n_q$. At each scale we expect that the number of cracks would depend on the stress, and furthermore, such dependence could be described by a self-similar function, i.e., a power law.

This directly leads to the conclusion that the number of active nanocracks that have a power-law dependence on the macroscale SIF [8,9] is $N_a \propto (K/K_{Ic})^p$, where $K_{Ic}=$ critical value of K at which the crack can propagate at monotonic loading. Therefore, Eq. (22) can be rewritten as

$$\dot{a}=A'e^{-Q_0/kT}\frac{K^{p+2}}{K_{Ic}^p} \quad (23)$$

where $A'=$ constant. For quasi-brittle structures, K_{Ic} is not a material constant, but varies with the structure size and geometry. Based on the energetic scaling of strength of quasi-brittle structures with a large pre-existing notch, the dependence of K_{Ic} on the structure size and geometry can be expressed as [5,45–47]

$$K_{Ic}=K_{I\infty}\left[\frac{D}{D+D_0}\right]^{1/2} \quad (24)$$

where $K_{I\infty}=$ fracture toughness, i.e., the value of K_{Ic} for infinitely large structures, and $D_0=$ transitional size. D_0 can be further related to the structural geometry: $D_0=g'(\alpha_0)c_f/g(\alpha_0)$ [2,46], where $g(\alpha)=$ dimensionless energy release rate function, $g'(\alpha)=\mathrm{d}g(\alpha)/\mathrm{d}\alpha$, $\alpha=$ relative crack length $=a/D$, and $c_f=$ effective size of FPZ. By substituting Eq. (24) into Eq. (23), one obtains a size- and geometry-dependent crack growth rate law:

$$\dot{a}=Ce^{-Q_0/kT}\left(1+\frac{D_0}{D}\right)^{\frac{n}{2}-1}K^n \quad (25)$$

where $C=A'K_{I\infty}^{2-n}$ and $n=p+2$. Comparing Eq. (25) with Eq. (20), it is clear that parameter A in Eq. (20) must depend on the structure size and geometry. Bažant and Xu [45] introduced a similar size effect to the Paris law for quasi-brittle structures under cyclic loading, and verified it by tests of the fatigue crack growth in concrete specimens of different sizes. Unfortunately, no experiments have yet been performed for the size dependence of static crack growth rate law.

Another noteworthy point is that, in the present model, the power-law exponent n is considered to be a constant. Extensive experiments showed that the power-law exponent of Paris law for fatigue crack growth could depend on the structure size and geometry [48,49]. However, the degree of such dependence varies for different materials and the corresponding mathematical description is unavailable. With the lack of experimental data on the size effect on the static crack growth rate, it is uncertain how the power-law exponent n would change with the structure size and geometry for quasi-brittle structures. Nevertheless, it may be pointed out that, in the present framework, the size dependence of the power-law exponent could be introduced by employing the argument of incomplete self-similarity for the function $N_a(K)$, which would be similar to Barenblatt and Botvina's concept of the size effect on the Paris law exponent [48,50].

Probability Distribution of Structural Lifetime

The kinetics of static crack growth will now be used to link the strength and the lifetime of one RVE. Consider that two tests are conducted on the same RVE: (1) The strength test, in which the RVE is directly loaded to failure and the failure stress σ_N is recorded, and (2) the lifetime test, in which the RVE is loaded under a prescribed nominal stress σ_0 and the loading duration λ is recorded. Here we consider that the RVE contains a subcritical

crack and fails when this crack propagates to its critical length. Within the framework of equivalent linear elastic fracture mechanics, this subcritical crack can be considered to represent the distributed damage in the RVE.

Applying Eq. (25) to the growth of the subcritical crack for the aforementioned two loading histories, one can obtain the relation between the strength and lifetime of one RVE:

$$\sigma_N = \beta \sigma_0^{n/(n+1)} \lambda^{1/(n+1)} \tag{26}$$

where $\beta = [r(n+1)]^{1/(n+1)}$ = constant and r = loading rate used in the strength test. Note that, in the present analysis, we apply the static crack growth rate to one RVE. Therefore the size dependence of crack growth rate is not a concern here.

Since the random strength and lifetime of one RVE are related by Eq. (26), the lifetime cdf of one RVE could be obtained by directly substituting Eq. (26) into Eqs. (5) and (6):

$$\text{for } \lambda < \lambda_{\text{gr}} : P_1(\lambda) = 1 - \exp\left[-(\lambda/s_\lambda)^{\bar{m}}\right] \tag{27}$$

$$\text{for } \lambda \geq \lambda_{\text{gr}} : P_1(\lambda) = P_{\text{gr}} + \frac{r_f}{\delta_G \sqrt{2\pi}} \int_{\gamma \lambda_{\text{gr}}^{1/(n+1)}}^{\gamma \lambda^{1/(n+1)}} e^{-(\lambda' - \mu_G)^2/2\delta_G^2} d\lambda' \tag{28}$$

where $\gamma = \beta \sigma_0^{n/(n+1)}$, $\lambda_{\text{gr}} = \beta^{-1} \sigma_0^{-n} \sigma_{N,\text{gr}}^{n+1}$, $s_\lambda = s_0^{n+1} \beta^{-(n+1)} \sigma_0^{-n}$, $P_{\text{gr}} = P_1(\lambda_{\text{gr}})$, and $\bar{m} = m/(n+1)$. It is clear that the lifetime cdf has a Weibull (power-law) tail and the remaining part of the cdf can be approximated as a Gaussian distribution transformed by a power law.

The lifetime of the structure is determined by the shortest lifetime of its RVEs. Therefore, the cdf of structural lifetime can again be calculated based on the weakest link model:

$$P_f(\sigma_0, \lambda) = 1 - \prod_{i=1}^{N} \{1 - P_1[\langle \sigma_0 s(\boldsymbol{x}_i) \rangle, \lambda]\} \tag{29}$$

where σ_0 = applied nominal stress = $c_n P/bD$ or = $c_n P/D^2$ for two- or three-dimensional scaling, and P = applied load. Similar to the strength cdf, it can easily be shown that the lifetime cdf of large-size structures must approach the Weibull distribution:

$$P_f(\lambda) = 1 - \exp\left[-\left(\int_V \langle s(\boldsymbol{x}_i) \rangle^{n\bar{m}} \frac{dV(\boldsymbol{x})}{V_0}\right), \left(\frac{\lambda}{s_\lambda}\right)^{\bar{m}}\right] \tag{30}$$

To calculate the lifetime cdf of small- or intermediate-size structures, we could use the same mathematical framework as that used for the cdf of strength. Either one could apply the nonlocal boundary layer method to numerically calculate the lifetime cdf, or use the Taylor expansion method to obtain an approximate closed-form expression of the lifetime cdf for structures with a simple stress field.

Scaling of Mean Structural Strength and Lifetime

The finite weakest-link model directly indicates that the type of strength cdf and lifetime cdf varies with the structure size and geometry. Consequently, it is expected that the mean structural strength and lifetime must also depend on the structure size and geometry. Figure 3 presents the calculated size effect curves of the mean strength and lifetime. It can be seen that the size effect curves converge to the classical Weibull size effect at the large size limit. For small- and intermediate-size structures ($N_{\text{eq}} < 1000$), the mean size effect curves deviate upward from the classical Weibull size effect. This is because the RVE size is not negligible compared to the structure size, where the classical Weibull distribution is inapplicable.

Although it is next to impossible to express the mean strength and lifetime in a closed form, approximate solutions can be obtained through asymptotic matching:

$$\bar{\sigma}_N = \left[\frac{N_a}{D} + \left(\frac{N_b}{D}\right)^{n_d \psi/m}\right]^{1/\psi} \tag{31}$$

$$\bar{\lambda} = \left[\frac{C_a}{D} + \left(\frac{C_b}{D}\right)^{n_d \varphi/m}\right]^{(n+1)/\varphi} \tag{32}$$

where n_d = number of spatial dimensions in which the structure is scaled, and N_a, N_b, ψ, m, C_a, C_b, φ, n are constants. Considering the large-size asymptotic limit, it is easy to conclude that m is the Weibull modulus of strength cdf, and n is the power-law exponent of the static crack growth rate. Constants N_a, N_b, ψ can be calibrated from three asymptotic conditions of the size effect curve of structural strength: $[\bar{\sigma}_N]_{D \to l_0}$, $[d\bar{\sigma}_N/dD]_{D \to l_0}$, and $\left[\bar{\sigma}_N D^{1/m}\right]_{D \to \infty}$. Similar asymptotic properties of the size effect curve of the mean lifetime can be used to identify C_a, C_b, φ.

Since the asymptotic properties of the mean size effect curves of strength and lifetime can be explicitly related to the strength and lifetime cdfs, the strength or lifetime cdf can thus be determined directly from the corresponding mean size effect. This is an attractive alternative to the conventional histogram testing. Compared to histogram testing, which requires hundreds of specimens, the mean size effect analysis requires merely tests of geometrically similar specimens with four sizes, with three to five specimens for each size.

Here we will outline this framework for the cdf of strength. To uniquely define the strength cdf, one would need four independent parameters, i.e., m, μ_G, P_{gr}, and s_0. At the large-size limit, Eq. (31) reduces to

$$\bar{\sigma}_N = (N_b/D)^{n_d/m} \tag{33}$$

On the other hand, the Weibull cdf of strength of large-size structures [Eq. (8)] gives the mean strength:

$$\bar{\sigma}_N = s_0 \Gamma(1 + 1/m) N_{\text{eq}}^{-1/m} \tag{34}$$

where $\Gamma(x)$ = gamma function. The Weibull modulus m can be determined by the slope of size effect curve at large-size limit. By comparing Eqs. (33) and (34), one can then determine s_0.

The remaining two constants μ_G and P_{gr} can be determined from two asymptotic conditions at the small-size limit. Based on Eq. (31) we have

$$\bar{\sigma}_N|_{D=l_0} = (N_a/l_0)^{1/\psi} \tag{35}$$

$$d\bar{\sigma}_N/dD|_{D=l_0} = \frac{1}{\psi}\left[-\frac{N_a}{l_0^2} + \frac{n_d \psi}{m}\left(\frac{N_b}{l_0}\right)^{n_d\psi/m-1}\right] \times \left[\frac{N_a}{l_0} + \left(\frac{N_b}{l_0}\right)^{n_d\psi/m}\right]^{1/\psi-1} \tag{36}$$

On the other hand, $[\bar{\sigma}_N]_{D \to l_0}$ and $[d\bar{\sigma}_N/dD]_{D \to l_0}$ can be expressed in terms of $P_1(\sigma_N)$:

$$\bar{\sigma}_N|_{D=l_0} = \int_0^\infty [1 - P_1(n_f)] dn_f = f_1(s_0, m, \mu_G, P_{\text{gr}}) \tag{37}$$

$$d\bar{\sigma}_N/dD|_{D=l_0} = -\int_0^\infty (dP_f/dD) d\bar{\sigma}_N \tag{38}$$

$$= -\frac{n_d D^{n_d-1}}{l_0^3} \int_0^\infty [P_1(\sigma_N) - 1] \ln[1 - P_1(\sigma_N)] d\sigma_N \tag{39}$$

$$= f_2(s_0, m, \mu_G, P_{\text{gr}}) \tag{40}$$

By comparing Eqs. (35) and (37) and Eqs. (36) and (40), we can obtain μ_G and P_{gr}. With the entire set of parameters for the cdf of

strength of one RVE, we can calculate the cdf of strength of structures of any size and geometry. Note that, to determine the lifetime cdf based on the mean size effect, the same framework can be applied except that one would need to know the power-law exponent of the static crack growth rate.

Optimum Fits of Strength and Lifetime Histograms

For decades, extensive efforts have been devoted to experimental investigations of strength and lifetime statistics of quasi-brittle materials through histogram testing [42,51–58]. A direct verification of the proposed model can be made by optimum fitting of the observed strength and lifetime histograms. It has been found that the strength and lifetime histograms of quasi-brittle materials, such as concrete, fiber composites, and industrial and dental ceramics, systematically deviate from a straight line on the Weibull scale. Instead, the histograms consist of two segments, where the lower part follows a straight line and the upper part deviates from the straight line to the right. Clearly, the two-parameter Weibull distribution could not fit these two segments simultaneously.

In contrast, the present theory predicts that the strength and lifetime cdfs must consist of two parts separated by the grafting probability: $P_g = 1-(1-P_{gr})^{N_{eq}}$. For $P_f \leq P_g$, the strength and lifetime distributions can be calculated as a chain of Weibullian elements, which leads to a Weibull cdf. For $P_f > P_g$, the strength cdf can be calculated as a chain of Gaussian elements and the lifetime cdf can be considered as a chain of elements with a Gaussian cdf transformed by a power law, which deviate from a straight line on the Weibull scale. Clearly this deviation is due to the fact that the RVE size is not negligible compared to the structure size (i.e., $P_g < 1$), and the grafting probability can be considered as a physical measure of the quasi-brittleness of the structures.

Figure 4 presents the optimum fits of strength and lifetime histograms of engineering ceramics. The details of tests are as follows: (a) Strength of silicon nitride with sintering additive ($Si_3N_4 - Al_2O_3 - Y_2O_3$) [58]: 27 specimens with dimensions $3 \times 4 \times 40$ mm were tested under four-point bending. (b) Strength of 99.9% Al_2O_3 [42]: four-point bending tests were carried out on 30 specimens with dimensions $4.5 \times 3.5 \times 45$ mm. (c) Lifetime of MgO-doped HPSN (hot-pressed silicon nitride): 25 specimens were tested under four-point bending at an elevated temperature 1100 °C. The applied stress is about 50% of the mean short-time strength. (d) Lifetime of 99.9% Al_2O_3: 25 specimens with dimensions $4.5 \times 3.5 \times 45$ mm were tested under four-point bending with an applied stress about 78% of the mean short-time strength. For four-point bend specimens, one could obtain a closed-form expression of the strength and lifetime cdfs based on the aforementioned Taylor expansion method.

As seen in Fig. 4, the present model agrees well with the experimentally measured strength and lifetime histograms. Further optimum fits of strength and lifetime cdf's of dental ceramic and fiber composites can be found in [8,9,59,60].

Failure Analysis of the Malpassets Dam

We will now apply the present theory to analyze the failure of the Malpasset Dam in the French Maritime Alps. Built in 1954, the dam failed at its first complete filling in 1959 [61–63]. The failure is believed to have been caused by vertical flexural cracks engendered by lateral displacement of abutment. The analysis may be simplified by considering only the midheight cross-sectional slice of the dam, which represents a horizontal circular two-hinge arch of constant thickness $H = 6.78$ m. The radius and central angle of the arch are $R = 92.68$ m and $2\beta = 133$ deg. The dam is loaded by the slip of its right abutment (Fig. 5).

To simplify the analysis of the failure of the Malpasset Dam in 1959, we assume the hydraulic pressure is resisted by a generic horizontal slice of the dam acting as an arch. To clarify the size effect, we consider geometrically similar two-dimensional arches of various dimensions D representing the depth of the arch (characteristic dimension of the arch to be scaled); R = radius of arch $= 13.67D$ (when $D = H$, the 2D arch model corresponds to the actual size of the Malpasset Dam). In this simplified two-dimensional arch model, the uniaxial stress can be conveniently

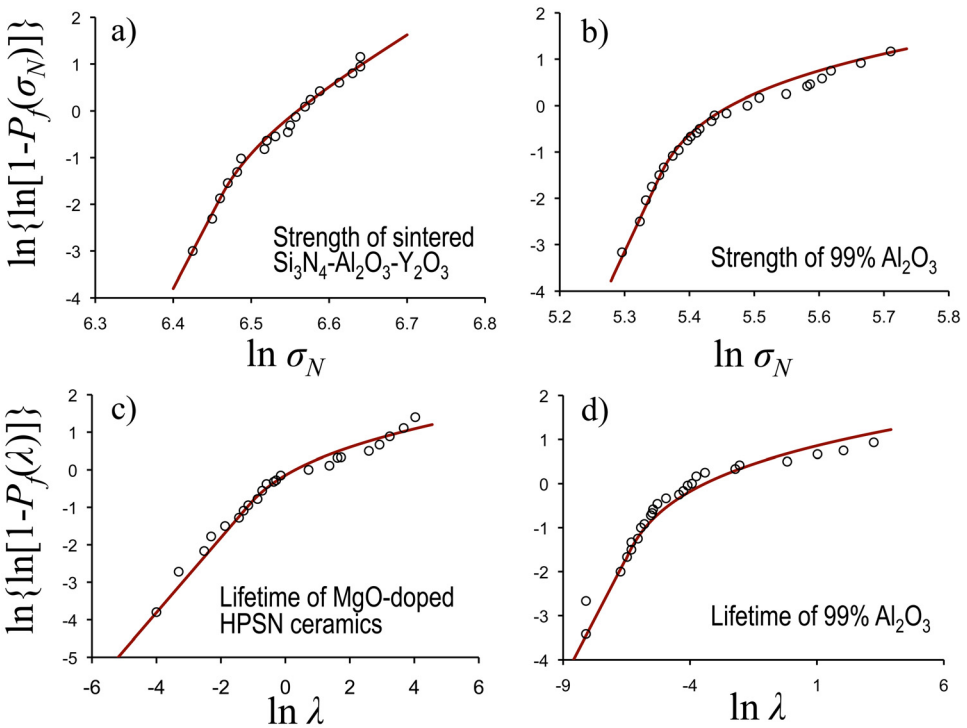

Fig. 4 Optimum fits of strength and lifetime histograms

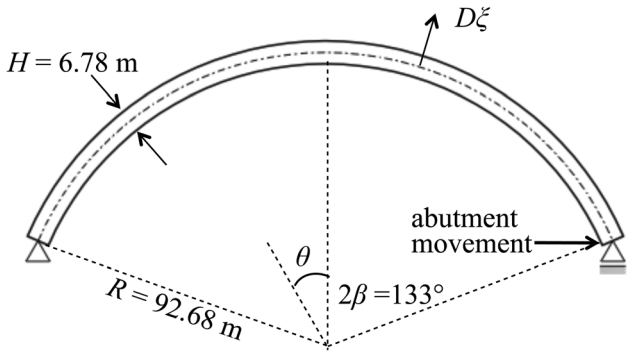

Fig. 5 Simplified 2D model of the Malpassets Dam

expressed in the polar coordinate ξ, θ (Fig. 5). The failure was caused by excessive lateral slip of the right abutment of the arch, denoted as u. From Castigliano's theorem and the classical theory of bending, the bending stress in the arch is

$$\sigma = \sigma_N \frac{2(\cos\beta - \cos\theta)\xi}{1 - \cos\beta} \tag{41}$$

$$\sigma_N = \frac{6u(1 - \cos\beta)}{CbD}\frac{R}{D} \tag{42}$$

where C = compliance $[\int_{-\beta}^{\beta} = (\cos\theta - \cos\beta)^2 d\theta] R^3/E$, E = elastic modulus, $\xi = y/D$, y = distance from the neutral axis, and σ_N is the maximal tensile stress, which occurs on the surface ($\xi = -1/2$) at the central cross section ($\theta = 0$).

Based on the simplified stress field, the cdf of nominal strength σ_N can be calculated by the nonlocal boundary layer method. The RVE size is chosen to be 0.28 m [64]. Considering geometrically similar arches of different sizes, we obtain the size effect on the mean nominal strength. By choosing proper statistical parameters, Fig. 6 shows that the mean size effect calculated on the basis of the present model agrees well with the recent stochastic finite element analysis of this arch by the microplane model for the actual size and scaled sizes [64]. Note that these two models start to deviate for small sizes for which there are only three to four RVEs across the arch depth. This is because when the structure is small the boundary layer occupies a large portion of the structure and the averaging of elastic strains within the boundary layer cannot realistically represent the actual stress redistribution in the deterministic calculation.

Figure 7 presents the size effect on the strength cdf. It can be seen that, for the generally accepted tolerable failure probability, which is $P_f \approx 10^{-6}$ [65–67], the corresponding nominal strength significantly decreases as the size of dam increases. For instance, compared to the strength of a prototype dam scaled down as 1:8, the nominal strength of the actual dam, which is proportional to its allowable abutment movement, is reduced by about 37%. The abutment movement considered in the design of this dam is not known but we can observe that if the size effect could have been considered in the design of this dam, the allowable movement of the abutment would have been 37% smaller than what was considered in design. Further note that this reduction corresponds to the case of deterministic loading. In reality, the abutment movement is uncertain and highly random. This means that a partial safety factor for the effect of abutment movement must be introduced as well, and according to the present theory this safety factor is also subjected to a size effect.

It is appropriate to comment on the role of failure statistics of microstructure in the analysis of large-scale structures such as the Malpasset Dam. In general, based on the present model, the size-dependent failure probability of the macrostructure is characterized by the Gauss-Weibull distribution of the macroscale RVE, which is based on the hierarchical series-parallel coupling model. The failure probability of the whole structure is then determined by a finite weakest-link model, whole links, corresponding to the individual RVEs, exhibit the Gauss-Weibull distribution of strength. However, the hierarchical model is only qualitative. It can predict the functional form of the strength distribution of each RVE, but not the values of its parameters. It is for this reason that, in the previous section, it is proposed to calibrate the Gauss-Weibull distribution from the macroscale mean size effect tests, which make it possible to identify the parameters of the Gauss-Weibull distribution of each RVE.

Salient Points and Conclusions

1. The only scale at which the probability of failure can be formulated exactly is the nanoscale. The reason is that the process of breakage of interatomic bonds is always quasi-stationary (in mechanics, though not in nuclear chain reaction). This implies that the probability of bond failure is exactly equal to the frequency of bond failure.

2. As shown herein, from one small set of a rather realistic hypotheses about the interatomic bond breakage and relatively plausible assumptions about the transition from nano- to macroscale, it is possible to derive the distribution of RVE strength, the scaling of this distribution with the structure size, the rate of static

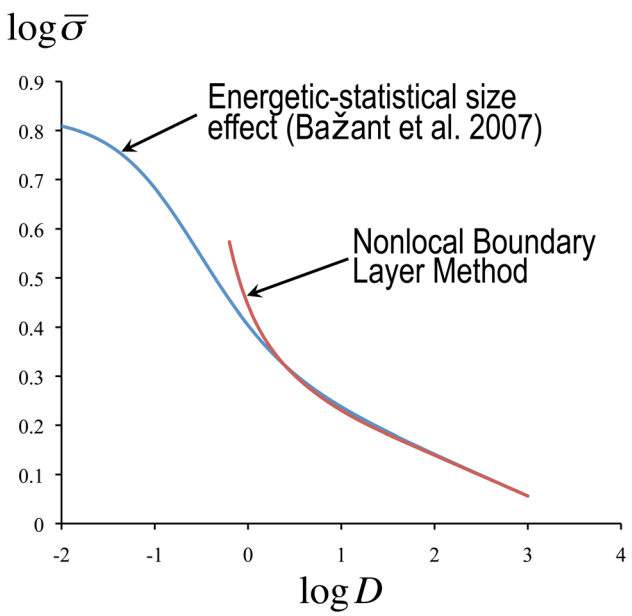

Fig. 6 Size effect on the mean nominal strength of the Malpassets Dam

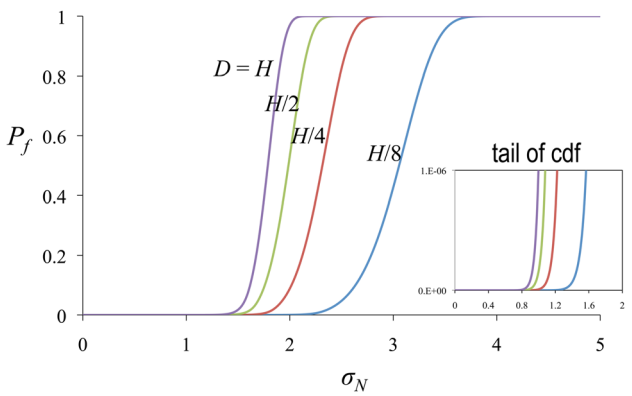

Fig. 7 Size effect on the cdf of nominal strength of the Malpassets Dam

crack propagation (Evans' law) on the RVE level, the distribution of the static lifetime, and the scaling of this distribution with the structure size. A separate paper [19] further shows that the rate of fatigue crack propagation (Paris law) on the RVE level, the distribution of the fatigue lifetime and its scaling with quasi-brittle structure size can be derived from the same hypotheses as well.

3. The main point for the scaling from one RVE to the structure size is that the chain model underlying the weakest-link statistics must be considered to have a *finite* number of links. This implies significant deviations from the Weibull distribution.

4. Failure analysis of the Malpasset Dam demonstrates the importance of size effect on the strength and lifetime cdfs in the design of large quasi-brittle structures.

Final Comment

Every brittle material becomes quasi-brittle on a sufficiently small scale at which the FPZ is no longer negligible compared to the cross section size. Thus it may be expected that the present finite weakest-link model would also be required for micrometer and submicrometer scale devices made from brittle materials.

Acknowledgment

The initial theoretical development was partially supported under Grant CMS-0556323 to Northwestern University (NU) from the U.S. National Science Foundation. The applications to concrete and to composites were partially supported by the U.S. Department of Transportation through the NU Infrastructure Technology Institute under Grant 27323, and also under Grant N007613 to NU from Boeing, Inc., respectively. The writing of this paper was supported by the Minnesota Department of Transportation through the Center of Transportation Studies at the University of Minnesota under Grant MN DOT/89261.

References

[1] Bažant, Z. P., 1984, "Size Effect in Blunt Fracture: Concrete, Rock, Metal," J. Eng. Mech., **110**(4), pp. 518–535.
[2] Bažant, Z. P., and Kazemi, M. T., 1990, "Determination of Fracture Energy, Process Zone Length and Brittleness Number From Size Effect, With Application to Rock and Concrete," Int. J. Fracture, **44**, pp. 111–131.
[3] Bažant, Z. P., and Kazemi, M. T., 1990, "Size Effect in Fracture of Ceramics and Its Use to Determine Fracture Energy and Effective Process Zone Length," J. Am. Ceram. Soc., **73**(7), pp. 1841–1853.
[4] Bažant, Z. P., 2004, "Scaling Theory of Quaisbrittle Structural Failure," Proc. Natl. Acad. Sci. U.S.A., **101**(37), pp. 13400–13407.
[5] Bažant, Z. P., 2005, *Scaling of Structural Strength*, 2nd ed., Elsevier, London.
[6] Bažant, Z. P., and Pang, S.-D., 2006, "Mechanics Based Statistics of Failure Risk of Quasibrittle Structures and Size Effect on Safety Factors," Proc. Natl. Acad. Sci. U.S.A., **103**(25), pp. 9434–9439.
[7] Bažant, Z. P., and Pang, S.-D., 2007, "Activation Energy Based Extreme Value Statistics and Size Effect in Brittle and Quasibrittle Fracture," J. Mech. Phys. Solids, **55**, pp. 91–134.
[8] Bažant, Z. P., Le, J.-L., and Bazant, M. Z., 2009, "Scaling of Strength and Lifetime Distributions of Quasibrittle Structures Based on Atomistic Fracture Mechanics," Proc. Natl. Acad. Sci. U.S.A., **106**(28), pp. 11484–11489.
[9] Le, J.-L., Bažant, Z. P., and Bazant, M. Z., 2011, "Unified Nano-Mechanics Based Probabilistic Theory of Quasibrittle and Brittle Structures: I. Strength, Static Crack Growth, Lifetime and Scaling," J. Mech. Phys. Solids, **59**, pp. 1291–1321.
[10] Bažant, Z. P., and Novák, D., 2001, "Nonlocal Model for Size Effect in Quasibrittle Failure Based on Extreme Value Statistics," *Proceedings of the 8th International Conference on Structural Safety and Reliability (ICOSSAR)*, R. B. Corotis, ed., Swets & Zeitinger, Balkema, pp. 1–8.
[11] Hillig, W. B., and Charles, R. J., 1964, "Surfaces, Stress-Dependent Surface Reaction, and Strength," *Proceedings of the 2nd Berkeley International Materials Conference*, V. F. Zackay, ed., J. Wiley, New Yotk.
[12] Wiederhorn, S. M., and Bolz, L. H., 1970, "Stress Corrosion and Static Fatigue of Glass," J. Am. Ceram. Soc., **53**(10), pp. 543–548.
[13] Evans, A. G., 1972, "A Method for Evaluating the Time-Dependent Failure Characteristics of Brittle Materials—and Its Application to Polycrystalline Alumina," J. Mater. Sci., **7**, pp. 1137–1146.
[14] Evans, A. G., and Fu, Y., 1984, "The Mechanical Behavior of Alumina," in *Fracture in Ceramic Materials*, Noyes Publications, Park Ridge, NJ, pp. 56–88.
[15] Thouless, M. D., Hsueh, C. H., and Evans, A. G., 1983, "A Damage Model of Creep Crack Growth in Polycrystals," Acta Metall., **31**(10), pp. 1675–1687.
[16] Fett, T., 1991, "A Fracture-Mechanical Theory of Subcritical Crack Growth in Ceramics," Int. J. Frac., **54**, pp. 117–130.
[17] Le, J.-L., Bažant, Z. P., and Bazant, M. Z., 2009, "Subcritical Crack Growth Law and Its Consequences for Lifetime Statistics and Size Effect of Quasibrittle Structures," J. Phys. D., **42**, p. 214008.
[18] Bažant, Z. P., and Le, J.-L., 2009, "Nano-Mechanics Based Modeling of Lifetime Distribution of Quasibrittle Structures," J. Eng. Failure Anal., **16**, pp. 2521–2529.
[19] Le, J.-L., and Bažant, Z. P., 2011, "Unified Nano-Mechanics Based Probabilistic Theory of Quasibrittle and Brittle Structures: II. Fatigue Crack Growth, Lifetime and Scaling," J. Mech. Phys. Solids, **59**, pp. 1322–1337.
[20] Abraham, F. F., Broughton, J. Q., Bernstein, N., and Kaxiras, E., 1998, "Spanning the Continuum to Quantum Length Scales in a Dynamical Simulation of Brittle Fracture," Europhys. Lett., **44**(6), pp. 783–787.
[21] Broughton, J. Q., Abraham, F. F., Bernstein, N., and Kaxiras, E., 1999, "Concurrent Coupling of Length Scales: Methodology and Application," Phys. Rev. B, **60**, pp. 2391–2403.
[22] Eyring, H., 1936, "Viscosity, Plasticity, and Diffusion As Examples of Absolute Reaction Rates," J. Chem. Phys., **4**, pp. 283–291.
[23] Glasstone, S., Laidler, K. J., and Eyring, H., 1941, *The Theory of Rate Processes*, McGraw-Hill, New York.
[24] Kramers H. A., 1941, "Brownian Motion in a Field of Force and the Diffusion Model of Chemical Reaction," Physica, **7**, pp. 284–304.
[25] Tobolsky, A., and Eyring, H., 1943, "Mechanical Properties of Polymeric Materials," J. Chem. Phys., **11**, pp. 125–134.
[26] Krausz, A. S., and Krausz, K., 1988, *Fracture Kinetics of Crack Growth*, Kluwer Academic, Netherlands.
[27] Kaxiras, E., 2003, *Atomic and Electronic Structure of Solids*, Cambridge University Press, Cambridge.
[28] Risken, H., 1989, *The Fokker-Plank Equation*, 2nd ed., Springer, Berlin.
[29] Philips, R., 2001, *Crystals, Defects and Microstructures: Modeling Across Scales*, Cambridge University Press, Cambridge.
[30] Redner, S., 2001, *A Guide to First-Passage Processes*, Cambridge University Press, Cambridge.
[31] Daniels, H. E., 1945, "The Statistical Theory of the Strength of Bundles and Threads," Proc. R. Soc. London Ser. A, **183**, p. 405–435.
[32] Coleman, B. D., 1958, "Statistics and Time Dependent of Mechanical Breakdown in Fibers," J. Appl. Phys., **29**(6), pp. 968–983.
[33] Harlow, D. G., and Phoenix, S. L., 1978, "The Chain-of-Bundles Probability Model for the Strength of Fibrous Materials I: Analysis and Conjectures," J. Comp. Mater., **12**, pp. 195–214.
[34] Phoenix, S. L., 1978, "Stochastic Strength and Fatigue of Fiber Bundles," Int. J. Frac., **14**(3), pp. 327–344.
[35] Harlow, D. G., Smith, R. L., and Taylor, H. M., 1983, "Lower Tail Analysis of the Distribution of the Strength of Load-Sharing Systems," J. Appl. Prob., **20**, pp. 358–367.
[36] Phoenix, S. L., Ibnabdeljalil, M., and Hui, C.-Y., 1997, "Size Effects in the Distribution for Strength of Brittle Matrix Fibrous Composites," Int. J. Solids Struct., **34**(5), pp. 545–568.
[37] Fisher, R. A., and Tippett, L. H. C., 1928, "Limiting Forms of the Frequency Distribution of the Largest and Smallest Member of a Sample," Proc. Cambridge Philos. Soc., **24**, pp. 180–190.
[38] Gumbel, E. J., 1958, *Statistics of Extremes*, Columbia University Press, New York.
[39] Ang, A. H.-S., and Tang, W. H., 1984,. *Probability Concepts in Engineering Planning and Design. Vol II. Decision, Risk and Reliability*, Wiley, New York.
[40] Haldar, A., and Mahadevan, S., 2000, *Probability, Reliability, and Statistical Methods in Engineering Design*, Wiley, New York.
[41] Bažant, Z. P., Le, J.-L., and Hoover, C. G., 2010, "Nonlocal Boundary Layer (NBL) Model: Overcoming Boundary Condition Problems in Strength Statistics and Fracture Analysis of Quasibrittle Materials," *Fracture Mechanics of Concrete and Concrete Structures—Recent Advances in Fracture Mechanics of Concrete*, B.-H. Oh, Ed., Korea Concrete Institute, Seoul, pp. 135–143.
[42] Munz, D., and Fett, T., 1999, *Ceramics: Mechanical Properties, Failure Behavior, Materials Selection*, Springer, Berlin.
[43] Lohbauer, U., Petchelt, A., and Greil, P., 2002, "Lifetime Prediction of CAD/CAM Dental Ceramics," J. Biomed. Mater. Res., **63**(6), pp. 780–785.
[44] Barenblatt, G. I., 1959, "The Formation of Equilibrium Cracks During Brittle Fracture, General Ideas and Hypothesis, Axially Symmetric Cracks," Prikl. Mater. Mech., **23**(3), pp. 434–444.
[45] Bažant, Z. P., and Xu, K., 1991, "Size Effect in Fatigue Fracture of Concrete," ACI Mater. J., **88**(4), pp. 390–399.
[46] Bažant, Z. P., and Planas, J., 1998, *Fracture and Size Effect in Concrete and Other Quasibrittle Materials*, CRC, Boca Raton, FL.
[47] Yu, Q., Le, J.-L., Hoover, C. G., and Bažant, Z. P., 2010, "Problems With Hu-Duan Boundary Effect Model and Its Comparison to Size-Shape Effect Law for Quasibrittle Fracture," J. Eng. Mech., **136**(1), pp. 40–50.
[48] Barenblatt, R. I., and Botvina, L. R., 1981, "Incomplete Self-Similarity of Fatigue in the Linear Range of Crack Growth," Fatigue Eng. Mater. Struct., **3**, pp. 193–212.
[49] Ritchie, R. O., 2005, "Incomplete Self-Similarity and Fatigue-Crack Growth," Int. J. Frac., **132**, pp. 197–203.
[50] Barenblatt, G. I., 2003, *Scaling*, Cambridge University Press, Cambridge.
[51] Weibull, W., 1939, "The Phenomenon of Rupture in Solids," Proc. R. Swedish Inst. Eng.Res., **153**, pp. 1–55.
[52] Chiao, C. C., Sherry, R. J., and Hetherington, N. W., 1977, "Experimental Verification of an Accelerated Test for Predicting the Lifetime of Organic Fiber Composites," J. Comp. Mater., **11**, pp. 79–91.
[53] Stanley, P., and Inanc, E. Y., 1985, "Assessment of Surface Strength and Bulk Strength of a Typical Brittle Material," in *Probabilistic Methods. I. The Mechanics of Solids and Structures*, S. Eggwertz and N. C. Lind, eds., Springer, Berlin, pp. 231–251.

[54] Fett, T., and Munz, D., 1991, "Static and Cyclic Fatigue of Ceramic Materials," in *Ceramics Today—Tomorrow's Ceramics*, P. Vincenzini, Ed., Elsevier Science, New York, pp. 1827–1835.
[55] Gross, B., 1996, "Least Squares Best Fit Method for the Three Parameter Weibull Distribution: Analysis of Tensile and Bend Specimens With Volume or Surface Flaw Failure," NASA TM-, 4721, pp. 1–21.
[56] Salem, J. A., Nemeth, N. N., Powers, L. P., and Choi, S. R., 1996, "Reliability Analysis of Uniaxially Ground Brittle Materials," ASME J. Eng. Gas Turbines Power, **118**, pp. 863–871.
[57] Tinschert, J., Zwez, D., Marx, R., and Ausavice, K. J., 2000, "Structural Reliability of Alumina-, Feldspar-, Leucite-, Mica- and Zirconia-Based Ceramics," J. Dent., **28**, pp. 529–535.
[58] Santos, C. d., Strecker, K., Piorino Neto, F., Silva, O. M. M, Baldacum, S. A., and da Filva, C. R. M., 2003, "Evaluation of the Reliability of Si_3N_4- Al_2O_3-CTR_2O_3 Ceramics Through Weibull Analysis," Mater. Res., **6**(4), pp. 463–467.
[59] Le, J.-L., and Bažant, Z. P., 2009, "Finite Weakest Link Model With Zero Threshold for Strength Distribution of Dental Restorative Ceramics," Dent. Mater., **25**(5), pp. 641–648.
[60] Pang, S.-D., Bažant, Z. P., and Le, J.-L., 2008, "Statistics of Strength of Ceramics: Finite Weakest Link Model and Necessity of Zero Threshold," Int. J. Frac., Special Issue on Physical Aspects of Scaling, **154**, pp. 131–145.
[61] Bartle, A., Ed., 1985, "Four Major Dam Failures Re-Examined," Int. Water Power Dam Constr., **37**(11), pp. 33–36, 41–46.
[62] Levy, M., and Salvadori, M., 1992, *Why Buildings Fall Down?*, W. W. Norton, New York.
[63] Pattison, K., 1998, "Why Did the Dam Burst?," Invention Technol., **14**(1), p. 2231.
[64] Bažant, Z. P., Vořechovský, M., and Novák, D., 2007, "Asymptotic Prediction of Energetic-Statistical Size Effect From Deterministic Finite Element Solutions," J. Eng. Mech., **128**, pp. 153–162.
[65] NKB, Nordic Committee for Building Structures, 1978, "Recommendation for Loading and Safety Regulations for Structural Design," NKB Report No. 36.
[66] Melchers, R. E., 1987, *Structural Reliability, Analysis & Prediction*, Wiley, New York.
[67] Duckett, K., 2005, "Risk Analysis and the Acceptable Probability of Failure," Struct. Eng., **83**(15), pp. 25–26.